Double stranded RNA-dependent protein kinase is necessary for TNF-α-induced osteoclast formation *in vitro* and *in vivo*

Hiroki Shinohara[1, 2], Jumpei Teramachi[1,*], Hirohiko Okamura[1], Di Yang[1], Toshihiko Nagata[2], and Tatsuji Haneji[1]

[1]Department of Histology and Oral Histology and [2]Department of Periodontology and Endodontology, Institute of Health Biosciences, The University of Tokushima Graduate School, Tokushima, Japan

Correspondence: Jumpei Teramachi, Department of Histology and Oral Histology, University of Tokushima Graduate School, 3-18-15, Kuramoto, Tokushima, 770-8504, Japan

Tel: +81-88-633-7322, Fax: +81-88-33-7342,

e-mail: jumptera@ tokushima-u.ac.jp

Running title: PKR is necessary for osteoclastogenesis.

Key words: PKR, osteoclast, RAW264.7, TNF-α, NF-κB, MAPK

Total text 28 pages and 7 figures

Grant sponsor: Ministry of Education, Science, Sports, and Culture of Japan; Grant number: 25861745 (JT) and 25462859 (TH).

ABSTRACT

Double-stranded RNA-dependent protein kinase (PKR) is involved in cell cycle progression, cell proliferation, cell differentiation, tumorgenesis, and apoptosis. We previously reported that PKR is required for differentiation and calcification in osteoblasts. TNF-α plays a key role in osteoclast differentiation. However, it is unknown about the roles of PKR in the TNF-α-induced osteoclast differentiation. The expression of PKR in osteoclast precursor RAW264.7 cells increased during TNF-α-induced osteoclastogenesis. The TNF-α-induced osteoclast differentiation in bone marrow-derived macrophages and RAW264.7 cells was markedly suppressed by the pre-treatment of PKR inhibitor, 2-aminopurine (2AP), as well as gene silencing of PKR. The expression of gene markers in the differentiated osteoclasts including TRAP, Calcitonin receptor, cathepsin K and ATP6V0d2 was also suppressed by the 2AP treatment. Bone resorption activity of TNF-α-induced osteoclasts was also supressed by 2AP treatment. Inhibition of PKR supressed the TNF-α-induced activation of NF-κB and MAPK in RAW264.7 cells. 2AP inhibited both the nuclear translocation of NF-κB and its transcriptional activity in RAW264.7 cells. 2AP inhibited the TNF-α-induced expression of NFATc1 and c-fos, master transcription factors in osteoclastogenesis. TNF-α-induced nuclear translocation of NFATc1 in mature osteoclasts was clearly inhibited by the 2AP treatment. The PKR inhibitor C16 decreased the TNF-α-induced osteoclast formation and bone resorption in mouse calvaria. The present study indicates that PKR is necessary for the TNF-α-induced osteoclast differentiation *in vitro* and *in vivo*.

INTRODUCTION

Double-stranded RNA-dependent protein kinase (PKR) is a serine/threonine protein kinase which is activated by double-stranded RNA (dsRNA), interferons, cytokines, stress signals, and viral infection [Cabanski et al., 2008; Sadler and Williams, 2008; Pindel and Sadler, 2011; Cachar et al., 2013; Liu et al., 2013]. PKR is also related to signal transduction pathways, such as mitogen-activated protein kinase (MAPK), nuclear factor of κB (NF-κB) and Smad [Morimoto et al., 2004, 2005; Takada et al., 2007; Nallagatla et al., 2011; Pfaller et al., 2011; Haneji et al., 2013]. We reported that PKR plays critical roles in bone formation and bone resorption as well as chondrogenesis [Yoshida et al., 2005, 2009; Teramachi et al., 2010; Morimoto et al., 2013].

The bone matrix is synthesized by osteoblasts whereas bone resorption is performed exclusively by osteoclasts and bone formation and bone resorption are closely balanced. Under the physiological conditions, bone tissue is constantly undergoing remodeling to achieve both calcium homeostasis and structural integrity. However, in the inflammatory diseases such as rheumatoid arthritis and periodontal disease, the balance between the activities of osteoblasts and osteoclasts are disrupted [Boyce, 2013; Khan et al., 2013; Lee et al., 2013]. TNF-α, one of the inflammatory cytokines, induces osteoclast differentiation and plays a role in progression of inflammatory bone destruction [Xu et al., 2009; Braun and Zwerina, 2011; Souza et al., 2013]. The pro-inflammatory effects of TNF-α are involved in osteo-immunological diseases [Kobayashi et al., 2014; Osta et al., 2014]. However, the roles of PKR in the TNF-α-induced osteoclast differentiation have not been investigated. In this study, we examined the roles of PKR in the TNF-α-induced osteoclast differentiation using PKR inhibitors, 2-aminopurine (2AP), or C16 as well as PKR gene interference. We demonstrate that treatment of 2AP suppressed osteoclastogenesis *in vitro*. Inhibition of PKR affects the pathway of NF-κB and MAPK and NFATc1 activation indicating that osteoclastogenesis was inhibited via downstream pathway of PKR. The present study also shows that inhibition of PKR by the treatment of the C16 PKR inhibitor decreased the TNF-α-induced bone destruction of mouse calvaria *in vivo*.

MATERIALS AND METHODS

Reagents

Alpha-modified Eagle minimal essential medium (α-MEM) was purchased from Gibco BRL (Grand Island, NY, USA). Fetal bovine serum (FBS) was purchased from JRH Biosciences (Lenexa, KS, USA). Recombinant mouse RANKL and M-CSF were purchased from PeproTech EC (London, UK). 2AP, MTT, and anti-β-actin antibody was obtained from Sigma-Aldrich (St. Louis, MO, USA). Anti-IκBα, anti-p38, anti-phosphorylated p38 (anti-p-p38), anti-ERK, and anti-phosphorylated ERK (anti-p-ERK) antibodies were obtained from Cell Signaling (Danvers, MA, USA). Anti-PKR (M-515), anti-NF-κB p50 (E-10), anti-NF-κB p65 (C-20), anti-NFATc1 (7A6), and anti-Eps15 antibodies were purchased from Santa Cruz Biotechnology (Santa Cruz, CA, USA). Anti-p84 antibody was obtained from abcam (Cambridge, MA, USA). TNF-α was purchased from WAKO (Osaka, Japan). The PKR inhibitor (C16) was purchased from Calbiochem (Darmstadt, Germany). Immobilon-P PVDF membrane and Immobilon Western were from Millipore (Medford, MA, USA). Plastic dishes were from IWAKI (Chiba, Japan). Other materials used were of the highest grade commercially available.

Differentiation of Osteoclasts

RAW264.7 cells were cultured in 96-well plates (750 cells per well) in α-MEM containing 10% FBS for 24 h in the presence of RANKL (25 ng/ml), the medium was removed and TNF-α (10 ng/ml) with various concentrations of 2AP were added. The cells were stained for TRAP after the 3 day cultivation and TRAP-positive multinucleated cells (MNCs) containing three or more nuclei were counted. Differentiated osteoclasts were also induced in bone marrow-derived macrophages (BMMs). Briefly, bone marrow cells were isolated from the tibia or femur of 5-week-old male C57BL/6J mice. The bone marrow cells ($2\text{-}3\times10^7$cells in a 10-cm dish) were cultured for 24 h in α-MEM containing 10% FBS. The non-adherent cells were collected and cultured for 3 days with 10 ng/ml of M-CSF. The adherent cells were referred to BMMs. For osteoclast generation, BMMs were pre-treated with 25 ng/ml of RANKL for 24 h; medium was removed and then stimulated with TNF-α for additional 3 days. To evaluate the effect of PKR inhibition on osteoclastogenesis, various concentrations of 2AP were added to these cultures for 3 h before TNF-α treatment. At the end of culture, the cells were fixed and stained for TRAP using a leukocyte acid phosphatase kit (Sigma-Aldrich). TRAP-positive MNCs containing three or more nuclei were counted.

MTT assay

Cell viability was measured by MTT assay. Mouse BMMs cultured for 3 days were incubated with MTT for 4 h, after removing media the cells were solubilized in dimethylformamide (DMSO). The absorbance at 595 nm was determined with a microplate reader.

Bone Resorption Assay

Mouse BMMs were cultured in Corning Osteo-Assay Surface 96-well plates (Corning, Lowell, MA, USA) in α-MEM containing 10% FBS and TNF-α in the presence or absence of 2AP. After 7 days of culture, the attached cells were removed from the slides using 6% sodium hypochlorite. The areas of dentin resorption were determined using image-analysis techniques (NIH Image J System).

Reverse Transcription PCR

RAW264.7 cells were cultured in six-well plates (1.5×10^5 cells per well) with RANKL for 24 h and the cells were treated with TNF-α for 48 h. Total cellular RNA was extracted using ISOGEN Reagent (Nippon GENE, Tokyo, Japan) and subjected to reverse transcription PCR (RT-PCR) using a RT-PCR kit (Takara Bio, Shiga, Japan). The primers used for PCR were as follows:

TRAP forward, 5'-CAGCTGTCCTGGCTCAAAA-3',

TRAP reverse, 5'-ACATAGCCCAGACCGTTCTC-3';

Calcitonin receptor (CTR) forward, 5’-TTTCAAGAACCTTAGCTGCCAGAG-3’,

CTR reverse, 5’- CAAGGCACGGACAATGTTGAGAG -3’;

Cathepsin K (CTK) forward, 5’-GAGGGCCAACTCAAGA-3’;

CTK reverse, 5’-GCCGTGGCGTTATACATACA-3’;

ATP6V0d2 forward, 5’-CAGATCTCTTCAAGGCTGTGCTG-3’;

ATP6V0d2 reverse, 5’-GTGCCAAATGAGTTCAGAGAGTGATG-3’;

PKR forward, 5’-GCCAGATGCACGGAGTAGCC-3’;

PKR reverse, 5’- GAAAACTTGGCCAAATCCACC -3’;

GAPDH forward, 5’-AAACCCATCACCATCTTCCA-3’ ;

GAPDH reverse, 5’-GTGGTTCACACCCATCACAA-3’

Following cDNA synthesis by reverse transcriptase, PCRs were carried out at 94°C for 30 sec, 55-60°C for 30 sec, and 72°C for 1 min (25-30 cycles). The PCR products were separated by electrophoresis on 2% agarose gels with ethidium bromide and visualized by UV light illumination.

Western Blotting

The cultured cells were collected and lysed in RIPA lysis buffer (Santa Cruz). For cytosolic and nuclear preparation, cells were lysed in NE-PER extraction reagent (Thermo Fisher Scientific, Waltham, MA, USA) according to the manufacturer’s protocol. The lysates containing equal amount of proteins were separated by 10% SDS-PAGE and transferred to PVDF membranes (Immobilon-P, Millipore). After blocking with 5% non-fat skim milk, the membranes were probed with optimally diluted primary antibodies overnight at 4°C followed by washing and incubation with peroxidase-conjugated second antibodies for 45 min at ambient temperature. Immunoreactive bands were visualized using Immobilon Western chemo luminescent system (Millipore). After stripping off the bound antibodies, the membranes were reproved with another antibody.

Small Interfering RNA (siRNA) Transfection

For transient silencing of PKR, RAW264.7 cells were transfected with 10 μg PKR small interfering RNA (sc-36264; Santa Cruz) using the siRNA Transfection Reagent (sc-29528; Santa Cruz, siPKR). Scrambled siRNA (sc-37007; Santa Cruz) was also transfected as a negative control (siCTL).

Luciferase Assay

NF-κB luciferase reporter was obtained from Stratagene (La Jolla, CA, USA). RAW264.7 cells were transfected with NF-κB reporter vector with the aid of Lipofectamine LTX™ reagent (Invitrogen, Carlsbad, CA, USA). GL3-basic vector (Promega, Madison, WI, USA) was used as the empty-vector control. The cells were treated with TNF-α in the presence or absence of 2AP for 24 h. The efficiency of the transfection was standardized by co-transfection with pTK-Renilla (Promega). Total cell lysates were prepared with the Dual-Glo® Luciferase Assay System (Promega) and assessed for luciferase activity.

Nuclear Localization of NF-κB and NFATc1

RAW264.7 cells were starved and treated for 30-90 min with 10 ng/ml of TNF-α. The cells were fixed for 10 min in 4% paraformaldehyde in PBS (PFA/PBS) at ambient temperature, washed in PBS, and permeabilized with 0.1% Triton X-100 for 5 min at ambient temperature. After blocking with 5% goat serum for 30 min, the cells were incubated with anti-p50 and p65 NF-κB antibodies and anti-NFATc1 antibody (1:100 in PBS; Santa Cruz) overnight at 4°C. The cells were washed in PBS and incubated with Alexa Fluor 594-conjugated anti-rabbit IgG and Alexa Fluor 488-conjugated anti-mouse IgG secondary antibodies (1:100 in PBS; Life technologies, Carlsbad, CA, USA) for 1 h at ambient temperature. After rinsing in PBS, the nuclei were stained with Hoechst 33342 (Dojindo, Kumamoto, Japan), and the fluorescent images were examined using a fluorescence microscope (BX50, Olympus, Tokyo, Japan).

[Ca^{2+}]i Oscillation

RAW264.7 cells (1×10^5 cells per 35 mm dish) were incubated with RANKL (25 ng/ml) for 24 h and then media were replaced with TNF-α (10 ng/ml) for another 24 h in the presence or absence of 2AP (5 mM). For intracellular Ca^{2+} measurement, cells were incubated with 5 μM fluo-4 AM and 0.05% pluronic F127 for 30 min in serum-free α-MEM, washed twice with Hanks' balanced salt solution (HBSS). At an excitation wavelength of 488 nm and emission at 520 nm for fluo-4 was analyzed simultaneously at 5 sec intervals using fluorescence microscope (Nikon). To estimate intracellular Ca^{2+} levels in single cell, the fluorescence intensity of fluo-4 AM from the basal level was calculated and expressed as the percent of maximum ratio increase, which was obtained by the addition of 10 μM ionomycin (Wako) at the end of experiments. Fluorescence intensity was analyzed by NIH Image J.

Micro-computed Tomography (μCT) and Histological Analyses

All animal experiments were conducted under the regulation and permission of the Animal Care and Use Committee of the University of Tokushima, Tokushima, Japan (toku-dobutsu 14054). Eight-week-old C57BL/6J mice were injected daily in the calvaria region with 10 μl of TNF-α (1.5 μg/μl), 10 μl of the PKR inhibitor (C16) (2.5 μg/μl) or PBS alone. After 7 days, mice were sacrificed, and craniums were dissected. Dissected mouse calvariae were fixed and analyzed by a μCT system (Latheta LCT-2000, Aloka, Tokyo, Japan). After μCT scanning, the craniums of mice were fixed overnight in 10% PFA/PBS, decalcified in 10% EDTA for 1 week at 4°C, and embedded in paraffin. Sections (3 μm) of samples were prepared and stained for TRAP activity. Bone histomorphometric parameters from calvariae were determined by measuring the areas at least 500 μm from the junction of the sagittal and coronal sutures. The percentage of osteoclast surface to bone surface (osteoclast perimeter) and eroded surface to bone surface (ES/BS) were obtained by measuring the areas of TRAP-positive cells and surface of the lacuna, respectively in serial 3-μm-thick coronal histological sections. TRAP-positive cells forming resorption lacunae on the surface of the bone and counting multiple nuclei were identified as osteoclasts.

Statistical analysis

All data are presented as means ± S.D. Statistical analysis was performed using Student's *t*-test or one-way analysis of variance (ANOVA). Results are representative examples of three or more independent experiments.

RESULTS

TNF-α increased the expression of PKR in osteoclast during *in vitro* differentiation.

RAW264.7 cells were pre-treated with RANKL (25 ng/ml) for 24 h to induce osteoclast generation, the medium was replaced with RANKL or TNF-α (10 ng/ml) for the indicated time periods. The cell lysates were prepared and the equal amounts of proteins were subjected to Western blot analysis. Figure 1 shows that RANKL and TNF-α increased the expression of PKR in the RANKL- pretreated RAW264.7 cells in a time-dependent manner up to 48 h. The level of β-actin did not change in these cells. In the cells treated with TNF-α, the level of PKR expression was greater than that in the cells treated with RANKL. The level of PKR expression in the RANKL pretreated cells stimulated with TNF-α increased 8-fold over that of the untreated cells; whereas the level of PKR expression in the cells treated with RANKL was 3-fold. RANKL and TNF-α also increased the expression of DC-STAMP and CTK in the cells undergoing osteoclastogenesis.

PKR inhibition suppressed the TNF-α-stimulated osteoclast formation *in vitro*

To determine the roles of PKR on the TNF-α-induced osteoclast formation, we examined the effects of 2AP, a specific inhibitor of PKR, on osteoclast formation. TRAP-positive cells were detected in the RANKL- pretreated primary BMM cell culture (Fig. 2Ab) in contrast to the cells without RANKL-stimulation (Fig. 2Aa). The formation of TRAP-positive osteoclast-like MNCs was accelerated in the cells treated with TNF-α (Fig. 2Ac). Treatment of 2AP decreased the formation of TRAP-positive

MNCs in the TNF-α-stimulated primary BMM cells in a dose-dependent manner (Figs. 2Ac-2Af). Quantitative analysis of the 2AP-inhibited osteoclastogenesis in primary BMM cells was shown in Figure 2B. There were no differences in the rate of cell proliferation in the 2AP-treated BMM cells indicating no cytotoxic effects of 2AP used in the present study (Fig. 2C).

Next, we examined the effects of 2AP on differentiation of RAW264.7 cells. Treatment of 2AP decreased the number of TRAP-positive MNCs in TNF-α-stimulated RAW264.7 cells (Fig. 3A). Quantitative analysis of the 2AP-inhibited osteoclastogenesis in RAW264.7 cells was also shown in Figure 3B. The expression of gene markers of differentiated osteoclasts, TRAP, CTR, CTK, and ATP6V0d2, was suppressed dose dependently with the 2AP treatment in the TNF-α-stimulated RAW264.7 cells (Fig. 3C). To confirm the roles of PKR in osteoclast formation, RAW264.7 cells were transfected with siRNA for PKR. First we confirmed the knockdown efficiency of PKR by RT-PCR and Western blotting. Figure 3D shows that the expression of PKR significantly decreased in the siPKR cells compared with that in siCTL. TNF-α stimulated the formation of TRAP-positive MNCs in the siCTL cells (Fig. 3Ea). However, the number of TRAP-positive MNCs was markedly decreased in the siPKR cells compared with that in the siCTL cells (Fig. 3Eb). Figure 3F shows the quantitative analysis of osteoclastogenesis in RAW264.7 cells transduced with siRNA.

2AP inhibited bone resorption activity.

We further investigated the effect of 2AP on the function of TNF-α-induced osteoclasts. RANKL-treated primary BMMs were cultured on hydroxyapatite-coated dishes with TNF-α in the presence or absence of 2AP, and bone resorption assay was performed.

TNF-α stimulated the formation of MNCs which performed pit formation on hydroxyapatite-coated dishes (Fig. 4). However, 2AP suppressed both the total number of pits (Fig. 4A) and the total area of resorption pits (Fig. 4B). The representative images of the pit formation were shown in Figure 4C. These results indicate that TNF-α-induced osteoclasts have bone resorption activity and that 2AP inhibited the function of the TNF-α-induced osteoclasts.

PKR inhibition potentiated TNF-α signaling pathway.

It is known that NF-κB and MAPK signaling pathways are important in osteoclast differentiation [Soysa and Alles, 2009]. To clarify the molecular mechanisms of PKR on TNF-α-induced osteoclastogenesis, we investigated whether PKR inhibition could affect these signaling pathways in RAW264.7 cells. TNF-α stimulated the phosphorylation of PKR, IκBα, p38 MAPK, and ERK (Fig. 5A). However 2AP decreased the levels of TNF-α-stimulated phosphorylation of these proteins, indicating that 2AP suppressed the TNF-α-stimulated activation of these signaling (Fig. 5A). Transient silencing of PKR by siRNA suppressed the phosphorylation of PKR and ERK, and the phosphorylation of IκB and p38 was partially inhibited compared to the control (Fig. 5B). RAW264.7 cells transfected with nonspecific siRNA were used as a control (siCTL). The levels of β-actin were used as loading control.

We analyzed the localization of NF-κB by immunostaining. In the untreated cells, p50 and p65 of NF-κB were mainly localized in the cytoplasm. However, nuclear translocation of p50 and p65 of NF-κB was observed in the cells treated with TNF-α (Fig. 5C). In contrast, NF-κB still localized in the cytoplasm in the cells treated with

2AP. To confirm the nuclear localization of NF-κB-p65, cytoplasmic and nuclear fractions were prepared and analyzed by Western blotting. In our culture system, the peak induction of nuclear translocation of p65 was observed around 30 to 60 min after TNF-α addition (Fig. 5D). To further examine the effect of 2AP on the NF-κB translocation, RAW264.7 cells were treated for 3 h with 2AP and incubated with TNF-α for 30 and 60 min. Increased expression of p65 was detected in the nuclear fraction of the TNF-α-treated cells but not in the 2AP treated cells (Fig. 5E). The purity of cytosolic and nuclear fractions was confirmed by the presence of Eps15 and p84, respectively (Figs. 5D and 5E). Results from the luciferase assay also indicated that 2AP suppressed the transcriptional activity of NF-κB (Fig. 5F).

2AP inhibited the TNF-α-induced expressions of NFATc1 and c-fos, nuclear translocation of NFATc1 and calcium signaling.

The expressions of c-fos and NFATc1 in RAW264.7 cells increased in the cells pretreated with RANKL. TNF-α further stimulated the expression of c-fos and NFATc1 in RAW264.7 cells after RANKL treatment. In contrast, 2AP strongly suppressed the levels of c-fos and NFATc1 expressions stimulated by TNF-α (Fig. 6A). The translocation of NFATc1 from the cytoplasm to the nucleus is reported to be the activation of osteoclast differentiation [Negishi-Koga and Takayanagi, 2009]. Mature osteoclasts formed from RAW264.7 cells were incubated with TNF-α for 90 min in the presence or absence of 2AP, and the localization of NFATc1 was examined by immunofluorescence. As shown in Figure 6B, TNF-α-treated cells showed obvious nuclear translocation of NFATc1. However, 2AP treatment suppressed the TNF-α-stimulated nuclear translocation of NFATc1. The quantitative analysis of the cells in which NFATc1 translocated in the nuclei was shown in Figure 6C.

It has been shown that Ca^{2+} oscillation is essential for the translocation of NFATc1, which is critical for the sustained NFATc1 nuclear translocation. We examined the effect of 2AP on Ca^{2+} oscillation in RAW264.7 cells stimulated with TNF-α. As shown in Figure 6D, TNF-α stimulated Ca^{2+} oscillation in RAW 264.7 cells (upper panel). The TNF-α-induced Ca^{2+} oscillation was markedly inhibited by 2AP-treatment (Fig. 6C, lower panel).

Osteoclast formation and bone resorption in mouse calvaria

We next examined the effects of PKR inhibition on the TNF-α-stimulated osteoclast formation *in vivo*. As shown in Figure 7A, when mice calvaria were injected with TNF-α for 7 days, bone density was significantly decreased, whereas in the PKR inhibitor C16-treated mice, the reduced bone density was abrogated. After μCT scan, mice calvaria was sliced and observed by TRAP staining. Osteoclast formation was induced in the TNF-α injected mouse calvaria compared with that of the control one (Fig. 7B). However, treatment of C16 markedly suppressed the TNF-α-stimulated osteoclast formation and bone resorption (Figs. 7B and 7C).

DISCUSSION

PKR is involved in cell cycle progression, cell proliferation, cell differentiation, tumorgenesis, and apoptosis [Jagus et al., 1999; Shogren et al., 2007; Haneji et al., 2013]. We have previously reported that PKR plays a critical role in differentiation of osteoblast [Yoshida et al., 2005], osteoclast [Teramachi et al., 2010], and chondrocyte [Morimoto et al., 2013]. However it is unknown about the role of PKR in the TNF-α-induced osteoclastogenesis. Previous report showed that various cytokines such as IFN-γ and TNF-α induce expression of PKR [Meurs et al., 1990]. Our present results showing that expression of PKR was induced during TNF-α-stimulated osteoclast formation suggest that PKR is necessary for osteoclastogenesis. We examined the role of PKR on TNF-α-induced osteoclast formation using 2AP, which is a specific inhibitor of PKR. For the inhibition experiment, we used 2AP at the concentrations up to 5 mM according to the previous report [Teramachi et al., 2010; Sugiyama et al., 2012; Morimoto et al, 2013]. The inhibitory effect of 2AP on osteoclast formation was not due to the cytotoxicity or reduced cell proliferation as shown in Figure 2C. Treatment of 2AP suppressed the TNF-α-induced TRAP-positive MNC formation in primary mouse BMM cells and osteoclast precursor RAW264.7 cells. The MNCs differentiated from BMM cells have osteoclastic activity because they performed pit formation on hydroxyapatite-coated dishes. These results indicate that PKR is involved in TNF-α-induced osteoclastogenesis. These findings are further supported by the fact that gene silencing of PKR inhibited the TNF-α-stimulated osteoclast formation in RAW264.7 cells.

It is well known that the stimulation of RANKL or TNF-α activates various signaling pathways including NF-κB, p38 MAPK, and ERK that are critical signaling for osteoclastogenesis [Lee and Kim, 2003]. PKR also regulates NF-κB, p38 MAPK, and ERK signaling [Bonnet et al., 2000; Takada et al., 2007; Nallagatla et al., 2011; Pfaller et al., 2011]. Therefore we examined whether PKR could mediate these signaling pathways in RAW264.7 cells stimulated with TNF-α. Inhibition of PKR activity with 2AP suppressed the degradation of IκBα and phosphorylation of p38 MAPK and ERK. These findings suggest that PKR is a pivotal factor for osteoclast differentiation by regulating NF-κB, p38MAPK, and ERK signaling. In the unstimulated cells, NF-κB is sequestered in the cytoplasm through an interaction with a family of inhibitory proteins, IκB. In the TNF-α-stimulated cells, the IκB protein is phosphorylated by IKK complex, then ubiquitinated and rapidly degraded, which leads to the nuclear translocation and activation of NF-κB proteins p50 and p65 [Karin and Lin, 2002]. However, inhibition of PKR activity blocked the translocation of NF-κB to the nucleus. Taken together, our results suggest that PKR is a critical mediator of TNF-α-induced NF-κB activation in osteoclastogenesis.

Activation of NF-κB and MAPK induces expressions of NFATc1 and c-fos in osteoclast precursors. Translocation of NFATc1 from the cytoplasm to the nucleus is essential for the expression of the associated genes with osteoclastogenesis [Huang et al., 2006; Zhao et al., 2010; Li et al., 2012]. We found that PKR inhibition suppressed the TNF-α-induced NFATc1 expression as well as nuclear translocation, resulting in the downregulation of the associated genes for osteoclast formation.

Translocation of NFATc1 is mainly regulated by Ca^{2+} signals. It was reported that auto-amplification of NFATc1 is regulated by calcineurin that mediates RANKL-induced Ca^{2+} oscillations during osteoclastogenesis [Takayanagi et al., 2002; Koga et al., 2004]. It was also reported that TNF-α induces calcium oscillations in human macrophages which is important for osteoclast formation [Yarilina et al., 2011]. However, the role of PKR on Ca^{2+} oscillation has not been previously reported.

Therefore, we examined whether PKR inhibition could affect Ca^{2+} oscillation induced by TNF-α. In our present study 2AP suppressed the TNF-α-induced intracellular Ca^{2+} oscillation in RAW264.7 cells. Other studies have shown that activation of ERK is also known to associate with calcium signaling [Wiegert et al., 2011]. In the present study, PKR inhibition suppressed the TNF-α-induced ERK activation. In osteoclast precursors, there could be some relationship between the alteration in the level of phosphorylation of ERK and the modulation of Ca^{2+} oscillation. However, further studies are required to determine the detailed molecular events concerning the suppression of TNF-α-induced Ca^{2+} oscillation by PKR inhibition.

Histological analysis of mouse calvaria clearly revealed that PKR inhibitor C16 prevents the TNF-α-stimulated osteoclast formation. These findings are strongly supported by our *in vitro* experiments in which PKR inhibition suppresses osteoclastogenesis through suppression of TNF-α-mediated signaling in osteoclast precursors. We previously demonstrated that differentiation of osteoblast and osteoclast did not occur in the PKR-dominant negative cells [Yoshida et al., 2005; Teramachi et al., 2010]. However, $PKR^{-/-}$ mice did not display any abnormalities in bone formation and resorption [Yang et al., 1995]. These results suggest that loss of PKR during development can be compensated by other molecules, which are yet to be identified.

In conclusion, we indicated that the expression of PKR increased during TNF-α-induced osteoclast formation. PKR plays a critical role in TNF-α induced osteoclast formation through regulating NF-κB, MAPK, and NFATc1 signaling pathways. We also demonstrated that PKR inhibition prevents TNF-α-induced bone destruction in vivo. Control of PKR activity may provide new therapeutic possibilities for the treatment of bone disease.

ACKNOWLEDGMENTS

We are thankful to Dr. Masayuki Shono for his help of Ca^{2+} oscillation assay. We also thank Ms. Eiko Sasaki for her skillful technical assistance. This study was supported in part by grants from the Grant-in-Aid for Scientific Research from the Ministry of Education, Science, Sports, and Culture of Japan (JT and TH).

LEGENDS TO FIGURES

Figure 1. The expression of PKR DC-STAMP and CTK in the TNF-α-induced osteoclast differentiation *in vitro*

RAW264.7 cells were pretreated with 25 ng/ml of RANKL for 24 h and then treated with RANKL or TNF-α (10 ng/ml) for the indicated time periods. The cell lysates were prepared, and equal amount of proteins were subjected to Western blot analysis with the specific antibodies for PKR, DC-STAMP, and CTK. The expression of β-actin was used as loading controls. The intensity of the immuno-positive bands from the blot was quantitated.

Figure 2. The role of PKR on osteoclast differentiation in mouse BMMs

(A) Primary mouse BMMs were cultured for 3 days with M-CSF to induce osteoclast precursors. The cells were pre-treated with RANKL for 24 h and cultured without (b) or with (c) TNF-α for 3 days. The RANKL- pretreated mouse BMMs were cultured with and TNF-α and 2AP at the concentrations of 1 mM (d), 2 mM (e), or 5 mM (f). The control cells are also represented (a). Bar represents 100 μm. (B) RANKL-pretreated mouse BMMs were cultured for 3 days with the indicated conditions followed by staining for TRAP. The numbers of TRAP-positive MNCs were counted. Data were analyzed by one-way ANOVA. *Significantly different from TNF-α treatment (*$p<0.05$). (C) Mouse BMMs are cultured for 3 days with various concentrations of 2AP. Cell viability was measured by MTT assay.

Figure 3. PKR inhibition suppressed the TNF-α-induced osteoclastogenesis in RAW264.7 cells.

(A) The RANKL- pretreated RAW264.7 cells were cultured for 3 days without (b) or with (c) TNF-α. The RANKL-pretreated RAW264.7 cells were also cultured with TNF-α and 5 mM 2AP (d). The control cells are also included (a). Bar represents 10 μm. (B) RAW264.7 cells were pre-treated with RANKL for 24 h and treated with TNF-α with various concentrations of 2AP for another 3 days. The number of TRAP-positive MNCs was counted. Data were analyzed by one-way ANOVA. *Significantly different from TNF-α treatment (*$P<0.05$). (C) RAW264.7 cells were stimulated to form osteoclast-like cells as described above. Total RNA was extracted and the levels of mRNA expression of the indicated genes were examined by RT-PCR. (D) Expression of PKR mRNA and protein in siRNA-transfected cells. The levels PKR mRNA and protein were examined by RT-PCR and Western blotting, respectively. Expression levels of GAPDH mRNA and β-actin protein were presented as the loading controls. (E) RANKL-pretreated siCTL (a) and siPKR (b) cells were cultured with

TNF-α for 3 days. Bar represents 5 μm. (F) The TRAP-positive MNCs were counted. *P<0.05 as determined by Student's *t*-test.

Figure 4. PKR inhibition suppresses bone resorption capacity.

The RANKL- pretreated and TNF-α-stimulated primary BMM cells were cultured with or without 2AP (5 mM) on osteo-assay plates for 7 days. The total numbers of resorption pits (A), total areas of resorption pits (B), and the image of pits (C) were analyzed as described in Materials and Methods. Data represent means ± SD, (n=4). Data were analyzed by Student's *t*-test. *P<0.05 compared with the culture without 2AP.

Figure 5. The roles of PKR on the TNF-α-induced signaling pathways and nuclear translocation of NF-κB

(A) RAW264.7 cells were starved in α-MEM containing 2% FBS for 16 h and incubated with or without 2AP for 3 h, followed by stimulation with TNF-α (10 ng/ml) for the indicated time periods. The cell lysates were prepared, and equal amount of proteins were subjected to Western blot analysis with the indicated antibodies. (B) Gene silencing of PKR suppressed the expression of PKR and inhibited phosphorylation of PKR, IκBα, p38, and ERK in RAW264.7 cells. (C) 2AP suppressed the TNF-α-induced nuclear translocation of NF-κB. RAW264.7 cells were incubated for 2 h with or without 2AP and then stimulated with TNF-α for 60 min. The cells were fixed and stained for NF- κ B-p50 (green) and p65 (red). Nuclei were stained with Hoechst 33342 (blue). The merged views were also shown. The bar represents 5 μm. (D) RAW264.7 cells were stimulated with TNF-α for the indicated periods. Cytosolic and nuclear fractions were prepared. Western blot analysis was performed using the NF-κB-p65 antibody. Eps15 and p84 were used as makers of cytosolic or nuclear fractions, respectively. (E) RAW264.7 cells were treated with TNF-α or 2AP for the indicated term and analyzed for Western blot with NF-κB-p65 antibody. Eps15 and p84 were used as makers of cytosolic or nuclear fractions, respectively. (F) 2AP suppressed the promoter activity of NF-κB. Cell lysates were collected from the cells treated with TNF-α and 2AP and then the luciferase activity was measured. Data are expressed relative to the value of sample from the control cells and values represent the means ± SD of representative analysis from 3 separate experiments. Data were analyzed by one-way ANOVA. *Significantly different from TNF-α treatment (* $p<0.05$, ** $p<0.01$).

Figure 6. The roles of 2AP on the TNF-α-induced c-fos and NFATc1 expressions and Ca^{2+} signaling.

(A) Expressions of c-fos and NFATc1 proteins in RAW264.7 cells. The cell lysates were prepared and subjected to Western blot analysis with the antibodies against c-fos, NFATc1, and β-actin. (B) 2AP suppressed the TNF-α-induced nuclear translocation of NFATc1. Mature osteoclasts from RAW264.7cells were incubated for 30 min with or without 2AP before TNF-α addition. The cells were fixed and stained for NFATc1 (green). Nuclei were stained with Hoechst 33342 (red). Merged views were shown (yellow). The photomicrograms of phase contrast were also shown in the left panels. The bars represent 10 μm. (C) 2AP suppressed the nuclear localization of NFATc1. Each value represents the percent of the cells in which NFATc1 localized in nucleus. The cells were counted in randomly selected 6 pictures. Data were analyzed by one-way ANOVA. *Significantly different from TNF-α treatment (*$p<0.05$, **$p<0.01$). n.s. (no significance). (D) 2AP treatment suppressed the TNF-α-induced Ca^{2+} oscillations in RAW264.7 cells. RANKL pre-treated cells were cultured with TNF-α (10 ng/ml) for 24 h in the absence (upper panel) or presence (lower panel) of 2AP (5 mM). $[Ca^{2+}]i$ change in single cell was detected by loading fluo-4 AM as described in Materials and Methods. Each color indicates corresponding single cells in the same field.

Figure 7. Induction of bone resorption with μCT analysis

(A) Three-dimensional μCT reconstruction images of mouse calvaria injected with PBS alone, TNF-α alone and TNF-α plus C16. Bar represents 3 mm. Arrowheads show the areas of low bone density. (B) Photomicrographs taken from sections of calvaria from mice injected with PBS alone, TNF-α alone, and TNF-α plus C16 and stained with TRAP as described in Materials and Methods. Arrowheads show TRAP-positive MNCs. Bar represents 100 μm. (C) Osteoclast perimeter measured in mice calvariae treated with PBS alone, TNF-α alone, and TNF-α plus C16. Data were analyzed by one-way ANOVA. *Significantly different from TNF-α treatment (*$p < 0.01$). n.s. (no significance).

REFERENCES

Bonnet MC, Weil R, Dam E, Hovanessian AG, Meurw EF. 2000. PKR stimulates NF-κB irrespective of its kinase function by interacting with the IκB kinase complex. Mol Cell Biol 20:4532-4542.

Boyce, BE. 2013. Advances in the regulation of osteoclasts and osteoclast function. J Dent Res 92:860-867.

Braun T, Zwerina J. 2011. Positive regulation of osteoclastogenesis and bone resorption in rheumatoid arthritis. Arthritis Res Ther 13:235.

Cabanski M, Steinmüller M, Marsh LM, Surdziel E, Seeger W, Lohmeyer J. 2008. PKR regulates TLR2/TLR4-dependent signaling in murine alveolar macrophages. Am J Respir Cell Mol Biol 38:26-31.

Cachat A, Chevalier SA, Alais S, Ko NL. 2013. Alpha interferon restricts human T-lymphotropic virus type 1 and 2 *de novo* infection through PKR activation. J Virol 87:2598-2635.Haneji T, Hirashima K, Teramachi J, Morimoto H. 2013. Okadaic acid activates PKR pathway and induces apoptosis through PKR-stimulation in osteoblastic MG63 cells. Int J Oncol 42:1904-1910.

Huang H, Chang EJ, Ryu J, Lee ZH, Lee Y, Kim HH. 2006. Induction of c-Fos and NFATc1 during RANKL-stimulated osteoclast differentiation is mediated by the p38 signaling pathway. Biochem Biophys Res Commun 351:99-105.

Jagus R, Joshi B, Barber GN. 1999. PKR, apoptosis and cancer. Int J Bio Chem 31:123-138.

Karin M, Lin A. 2002. NF-κB at the crossroad of life and death. Nat Immunol 3:211-217.

Khan UA, Hashimi SM, Bakr MM, Forwood MR, Morrison NA. 2013. Foreign body giant cells and osteoclasts are TRAP positive, have podosome-belts and both require DC-STAMP for cell fusion. J Cell Biochem 114:1772-1778.

Kobayashi T, Yokoyama T, Ito S, Kobayashi D, Yamagata A, Okada M, Oofusa K, Narita I, Murasawa A, Nakazono K, Yoshie H. 2014. Periodontal and serum protein profiles in patients with rheumatoid arthritis treated with tumor necrosis factor inhibitor Adalimumab: J Periodontl 26:1-9.

Koga T, Inui M, Inoue K, Kim S, Suematsu A, Kobayashi E, Iwata T, Ohnishi H, Matozaki T, Kodama T, Taniguchi T, Takayanagi H, Takai T. 2004. Costimulatory signals mediated by the ITAM motif cooperate with RANKL for bone homeostasis. Nature 428:758-763.

Lee ZH, Kim HH, 2003. Signal transduction by receptor activator of nuclear factor kappa B in osteoclasts. Biochem Biophys Res Commun 305:211-214.

Lee SK, Chung JH, Choi SC, Auh QS, Lee YM, Lee SI, Kim EC. 2013. Sodium hydrogen sulfide inhibits nicotine and lipopolysaccharide-induced osteoclastic differentiation and reversed osteoblastic differentiation in human periodontal ligament cells. J Cell Biochem 114:1183-1193.

Li YJ, Kukita A, Watanabe T, Takano T, Qu P, Sanematsu K, Ninomiya Y, Kukita T. 2012. Nordihydroguaiaretic acid inhibition of NFATc1 suppresses osteoclastogenesis and arthritis bone destruction in rats. Lab Invest 92:1777-1787.

Liu X, Bennett RL, Cheng X, Byrne M, Reinhard MK, May WS Jr. 2013. PKR regulates proliferation, differentiation, and survival of murine hematopoietic stem/progenitor cells. Blood 121:3364-3374

Meurs E, Chong KL, Galabru J, Thomas NS, Ken IM, Williams BR, Hovanessian AG. 1990. Molecular cloning and characterization of the human double-stranded RNA activated protein kinase induced by interferon. Cell 62:379-390.

Morimoto H, Okamura H, Yoshida K, Kitamura S, Haneji T. 2004. Okadaic acid induces apoptosis through double-stranded RNA-dependent protein kinase/eukaryotic initiation factor-2α pathway in human osteoblastic MG63 cells. J Biochem 136: 433-438.

Morimoto H, Ozaki A, Okamura H, Yoshida K, Kitamura S, Haneji T. 2005. Okadaic acid induces tyrosine phosphorylation of IκBα that mediated by PKR pathway in human osteoblastic MG63 cells. Mol Cell Biochem 276: 211-217.

Morimoto H, Baba R, Haneji T, Doi Y. 2013. Double-stranded RNA dependent protein kinase regulates insulin-stimulated chondrogenesis in mouse clonal chondrogenic cells ATDC-5chondrogenesis in mouse clonal chondrogenic cells, ATDC-5. Cell Tissue Res 351:41-47.

Nallagatla SR, Toroney R, Bevilacqua PC. 2011. Regulation of innate immunity through RNA structure and the protein kinase PKR. Curr Opin Struct Biol 21:119-127.

Negishi-Koga T, Takayanagi H. 2009. Ca^{2+}-NFATc1 signaling is an essential axis of osteoclast differentiation. Immunol Rev 231:241-256.

Osta B, Benedetti G, Miossec P. 2014. Classical and paradoxical effects of TNF-α on bone homeostasis. Front Immunol 5:48. eCollection

Pfaller CK, Li Z, George CX, Samuel CE. 2011. Protein kinase PKR and RNA adenosine deaminase ADR1: new roles for old players as modulators of the interferon response. Curr Opin Immunol 23:573-582.

Pindel A, Sadler AJ. 2011. The role of protein kinase R in the interferon responses. J Interferon Cytokine Res 31:59-70.

Sadler AJ, Williams BRG. 2008. Interferon-inducible antiviral effectors. Nat Rev

Immunol 8:559-568.

Shogren KL, Turner RT, Yaszemski MJ, Maran A. 2007. Double-stranded RNA-dependent protein kinase is involved in 2-methoxyestradiol-mediated cell death of osteosarcoma cells. J Bone Miner Res 22:29-36.

Souza PP, Lerner UH. 2013. The role of cytokines in inflammatory bone loss. Immunol Invest 42:555-622.

Soysa NS, Alles N. 2009. NF-κB functions in osteoclasts. Biochem Biophys Res Commun 378:1-5.

Sugiyama T, Gotou T, Moriyama K, Kajiura N, Hasegawa T, Tomida J, Takahashi K, Komatsu T, Ueda H, Sato K, Tokoro S, Neri P, Mori H. 2012. Mechanism of inhibition of lipopolysaccharide-induced interferon-β production by 2-aminopurine. Mol Immunol 52:299-304.

Takada Y, Ichikawa H, Pataer A, Swisher S, Aggarwal BB. 2007. Genetic deletion of PKR abrogates TNF-induced activation of IκBα kinase, JNK, Akt and cell proliferation but potentiates p44/p42 MAPK and p38 MAPK activation. Oncogene 26:1201-1212.

Takayanagi H, Kim S, Koga T, Nishina H, Isshiki M, Yoshida H, Saiura A, Isobe M, Yokochi T, Inoue J, Wagner EF, Mak TW, Kodama T, Taniguchi T. 2002. Induction and activation of the transcription factor NFATc1 (NFAT2) integrate RANKL signaling in terminal differentiation of osteoclasts. Dev Cell 3:889-901.

Teramachi J, Morimoto H, Baba R, Doi Y, Hirashima K, Haneji T. 2010. Double stranded RNA-dependent protein kinase is involved in osteoclast differentiation of RAW264.7 cells in vitro. Exp Cell Res 316:3254-3262.

Wiegert JS, Bading H. 2011. Activity-dependent calcium signaling and ERK-MAP kinases in neurons: a link to structural plasticity of the nucleus and gene transcription regulation. Cell Calcium 49:296-305.

Xu J, Wu HF, Ang ES, Yip K, Woloszyn M, Zheng MH, Tan RX. 2009. NF-κB modulators in osteolytic bone diseases. Cytokine Growth Factor Rev 20:7-17.

Yang YL, Reis LF, Pavlovic J, Aguzzi A, Schäfer R, Kumar A, Williams BR, Aquet M, Weissmann C. 1995. Deficient signaling in mice devoid of double-stranded RNA-dependent protein kinase. EMBO J 14:6095-6106.

Yarilina A1, Xu K, Chen J, Ivashkiv LB. 2011. TNF activates calcium-nuclear factor of activated T cells (NFAT)c1 signaling pathways in human macrophages. Proc Natl Acad Sci USA 108:1573-1578.

Yoshida K, Okamura H, Amorim BR, Ozaki A, Tanaka H, Morimoto H, Haneji T. 2005. Double-stranded RNA-dependent protein kinase is required for bone calcification in MC3T3-E1 cells in vitro. Exp Cell Res 311:117-125.

Yoshida K, Okamura H, Amorim BR, Hinode D, Yoshida H, Haneji T. 2009. PKR-mediated degradation of STAT1 regulated osteoblast differentiation. Exp Cell Res 315:2105-2114.

Zhao Q, Wang X, Liu Y, He A, Jia R. 2010. NFATc1: functions in osteoclasts. Int J Biochem Cell Biol 42:576-579.

Fig.1.

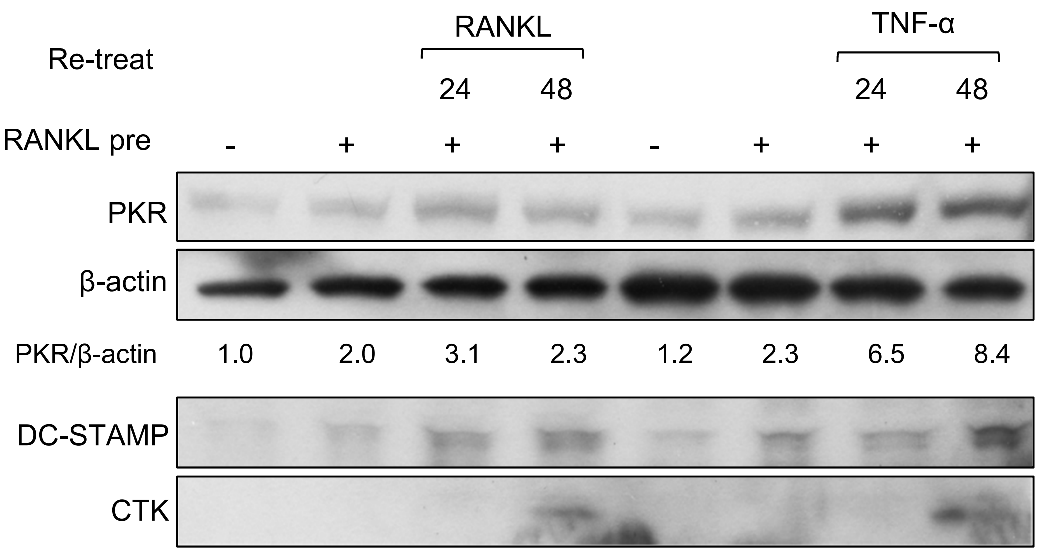

RANKL
TNF-α
Re-treat
24
48
24
48
RANKL pre
-
+
+
+
-
+
+
+
PKR
β-actin
PKR/β-actin
1.0
2.0
3.1
2.3
1.2
2.3
6.5
8.4
DC-STAMP
CTK

Fig.2.

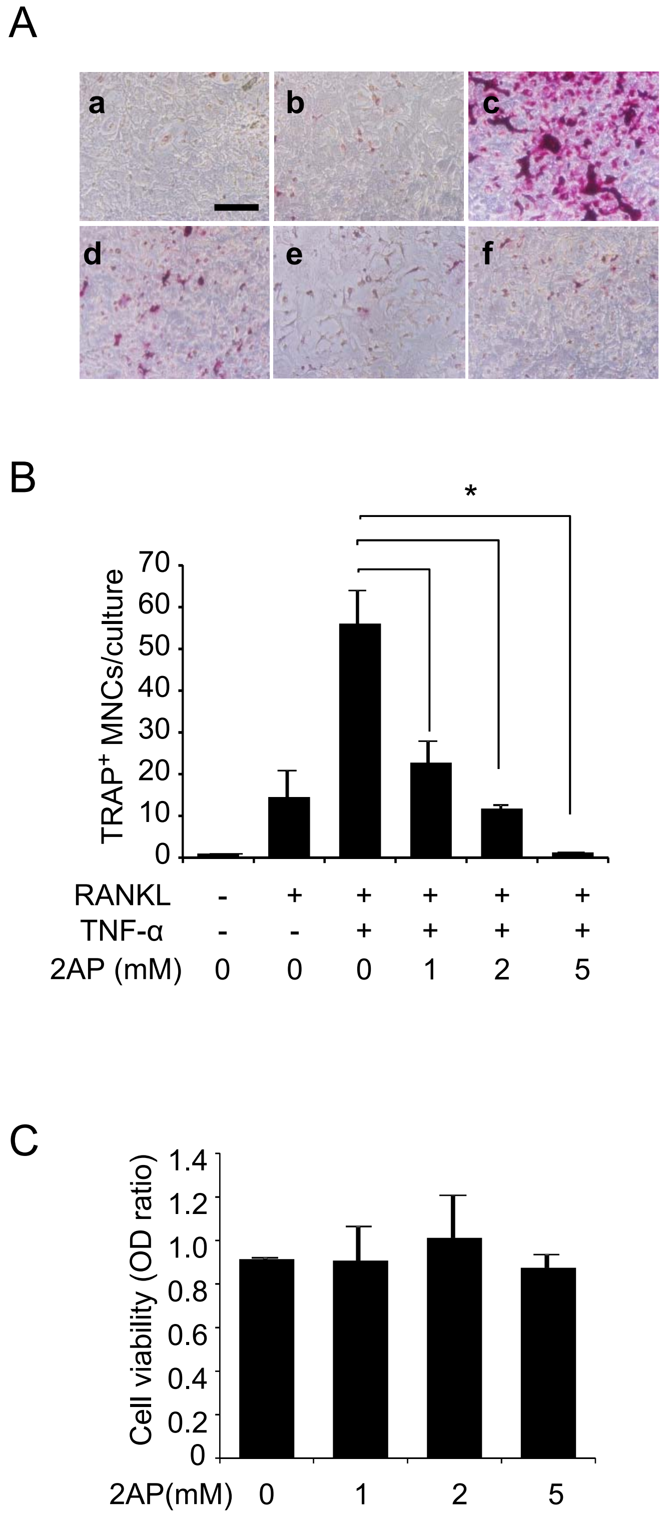
A
a
b
c
d
e
f
B
*
TRAP+ MNCs/culture
70
60
50
40
30
20
10
0
RANKL - + + + + +
TNF-α - - + + + +
2AP (mM) 0 0 0 1 2 5
C
Cell viability (OD ratio)
1.4
1.2
1.0
0.8
0.6
0.4
0.2
0
2AP(mM) 0 1 2 5

Fig.3.

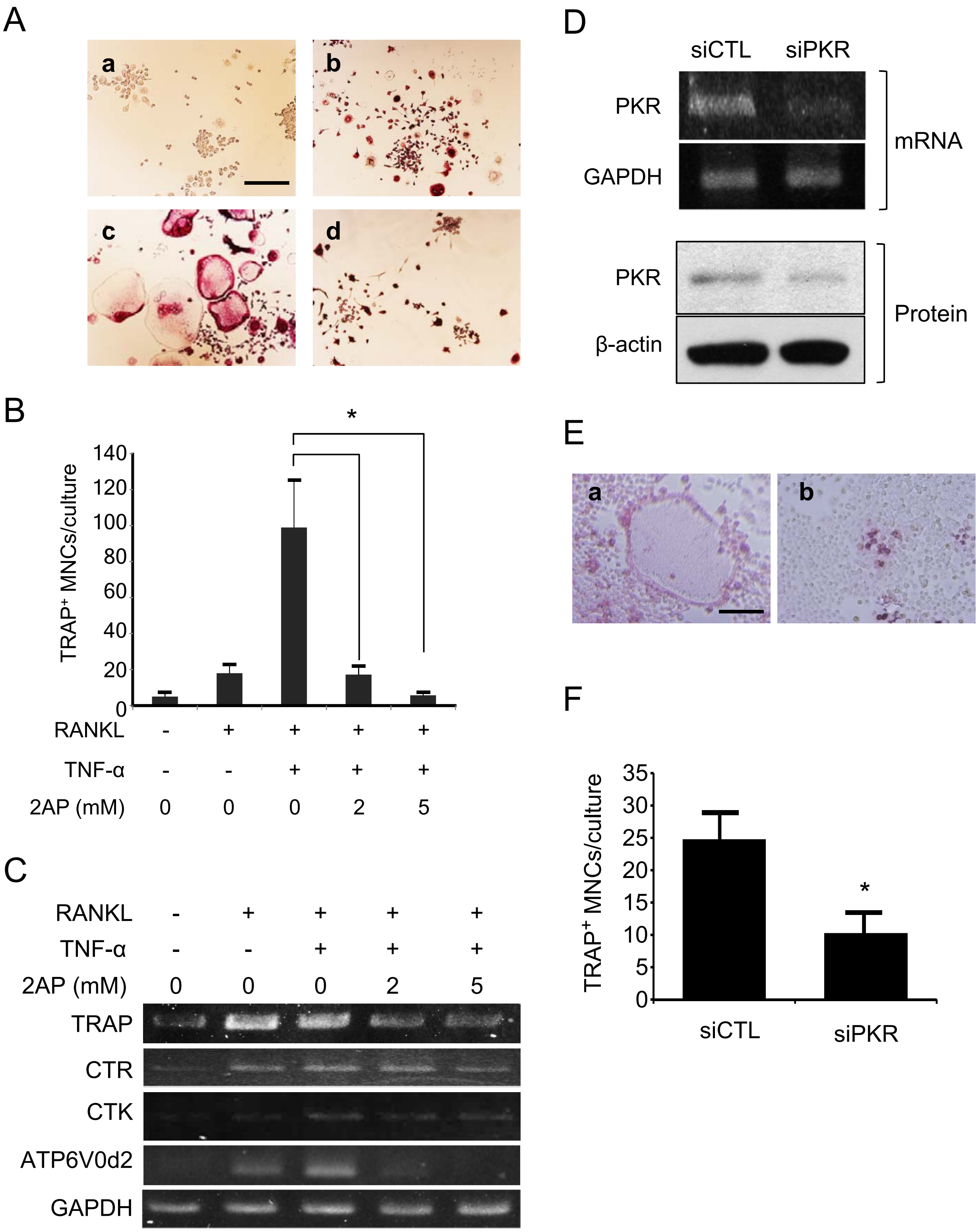
A
a
b
c
d
B
*
TRAP⁺ MNCs/culture
140
120
100
80
60
40
20
0
RANKL - + + + +
TNF-α - - + + +
2AP (mM) 0 0 0 2 5
C
RANKL - + + + +
TNF-α - - + + +
2AP (mM) 0 0 0 2 5
TRAP
CTR
CTK
ATP6V0d2
GAPDH
D
siCTL siPKR
PKR
GAPDH
mRNA
PKR
β-actin
Protein
E
a
b
F
TRAP⁺ MNCs/culture
35
30
25
20
15
10
5
0
*
siCTL
siPKR

Fig.4.

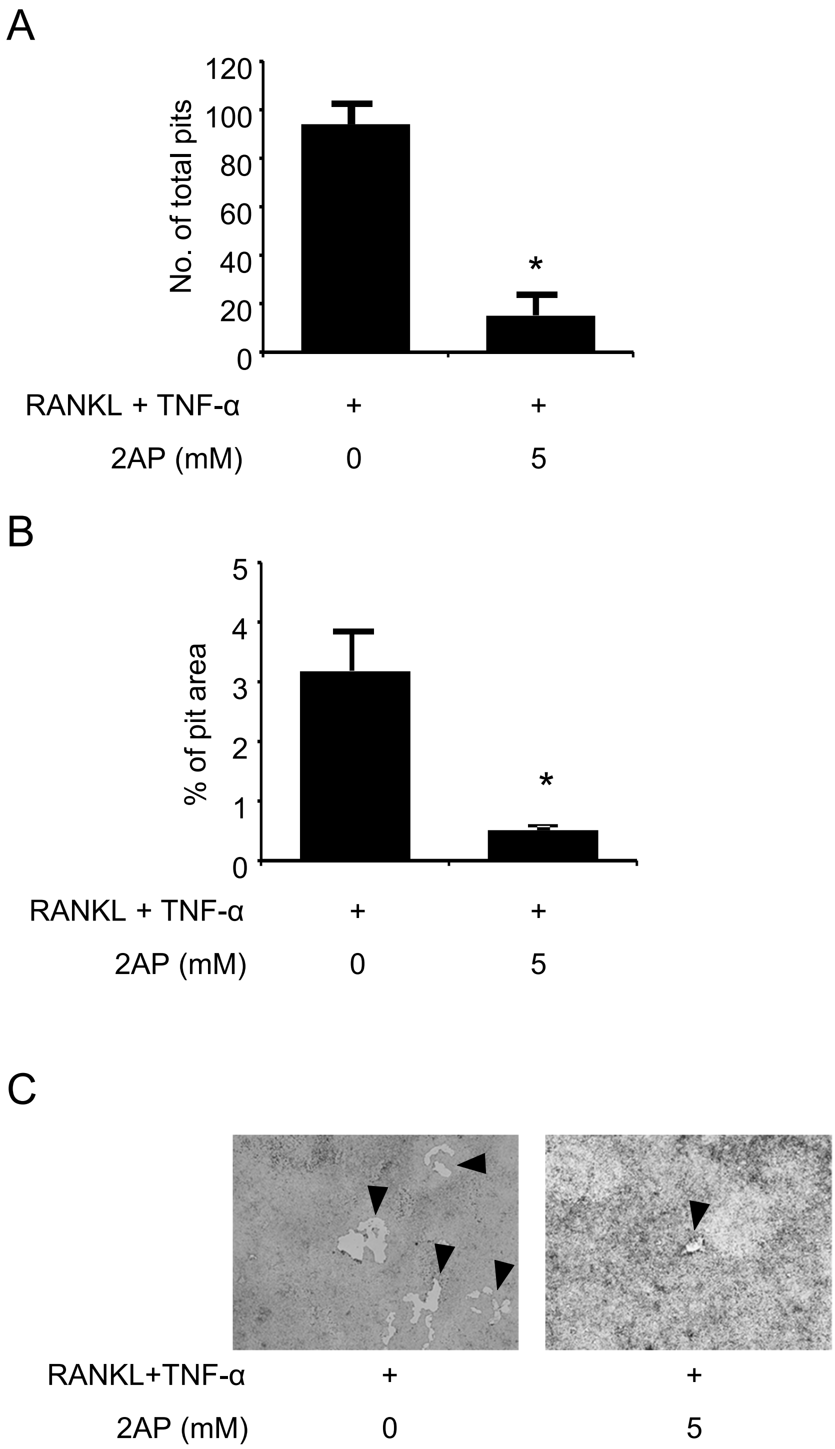
A
No. of total pits
120
100
80
60
40
20
0
*
RANKL + TNF-α + +
2AP (mM) 0 5
B
% of pit area
5
4
3
2
1
0
*
RANKL + TNF-α + +
2AP (mM) 0 5
C
RANKL+TNF-α + +
2AP (mM) 0 5

Fig.5.

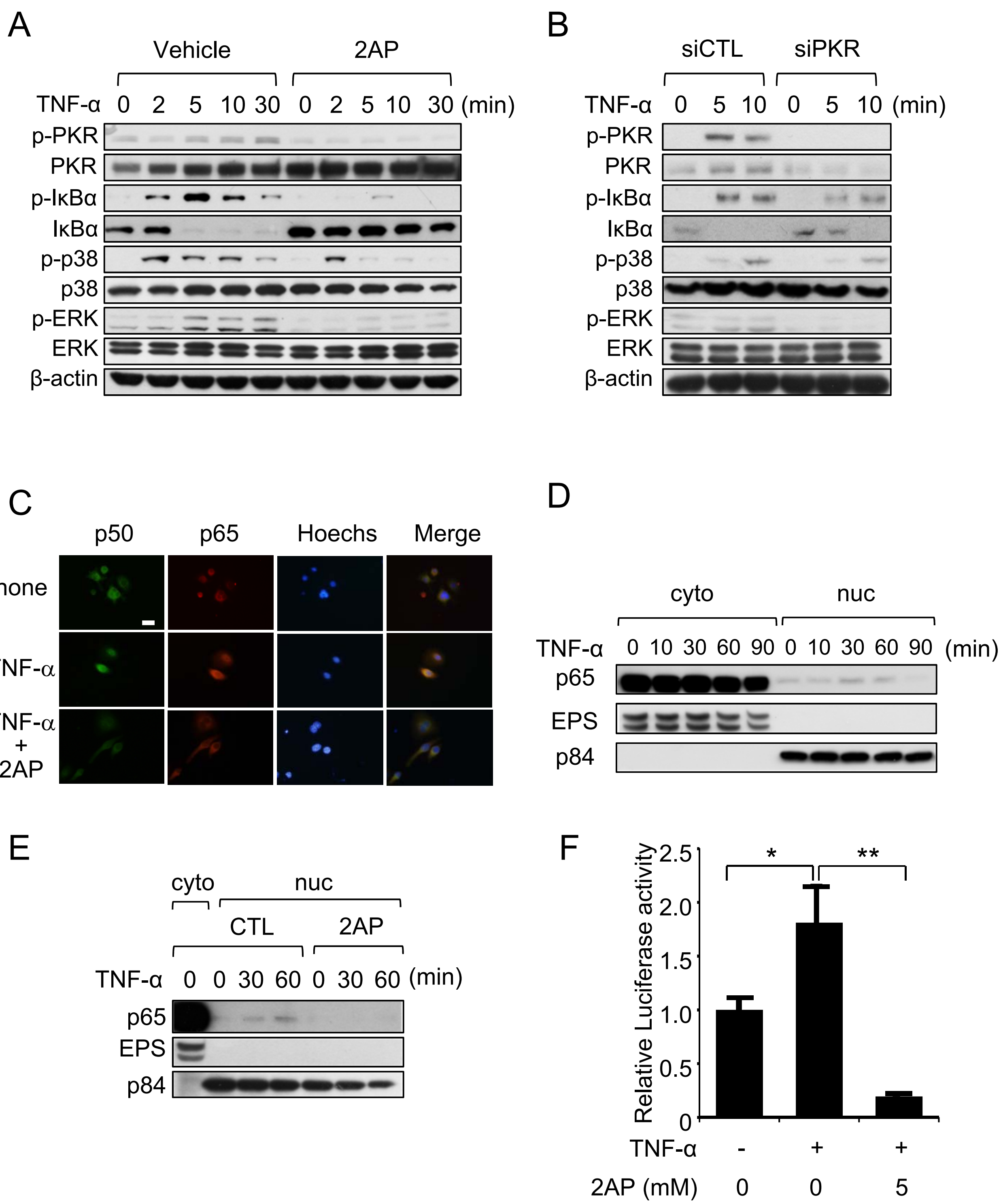
A
Vehicle
2AP
TNF-α 0 2 5 10 30 0 2 5 10 30 (min)
p-PKR
PKR
p-IκBα
IκBα
p-p38
p38
p-ERK
ERK
β-actin
B
siCTL
siPKR
TNF-α 0 5 10 0 5 10 (min)
p-PKR
PKR
p-IκBα
IκBα
p-p38
p38
p-ERK
ERK
β-actin
C
p50
p65
Hoechs
Merge
none
TNF-α
TNF-α + 2AP
D
cyto
nuc
TNF-α 0 10 30 60 90 0 10 30 60 90 (min)
p65
EPS
p84
E
cyto
nuc
CTL
2AP
TNF-α 0 0 30 60 0 30 60 (min)
p65
EPS
p84
F
Relative Luciferase activity
2.5
2.0
1.5
1.0
0.5
0
*
**
TNF-α - + +
2AP (mM) 0 0 5

Fig.6.

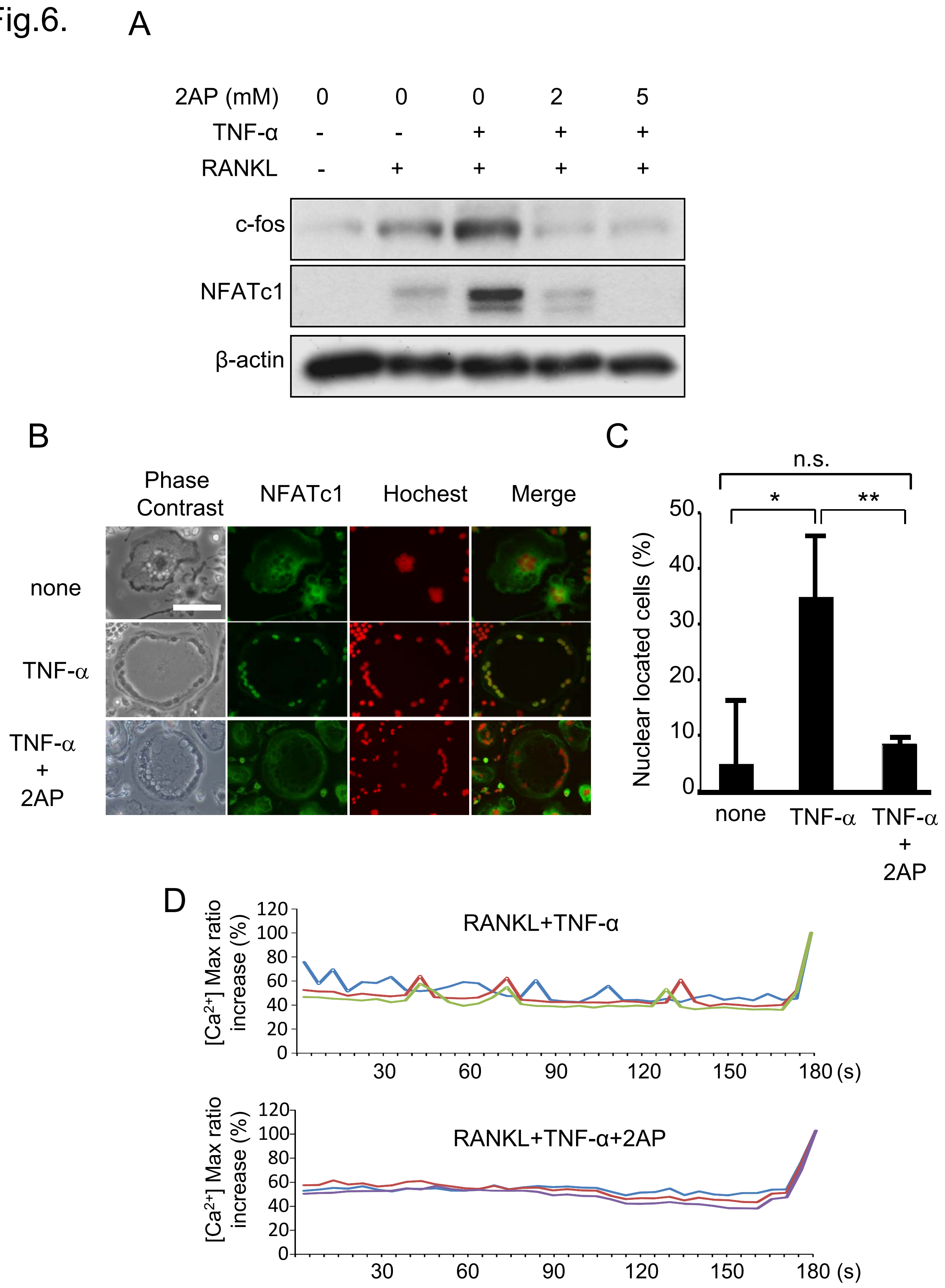
A
2AP (mM) 0 0 0 2 5
TNF-α - - + + +
RANKL - + + + +
c-fos
NFATc1
β-actin
B
Phase Contrast
NFATc1
Hochest
Merge
none
TNF-α
TNF-α + 2AP
C
n.s.
*
**
Nuclear located cells (%)
50
40
30
20
10
0
none
TNF-α
TNF-α + 2AP
D
RANKL+TNF-α
[Ca2+] Max ratio increase (%)
120
100
80
60
40
20
0
30
60
90
120
150
180 (s)
RANKL+TNF-α+2AP

Fig.7.

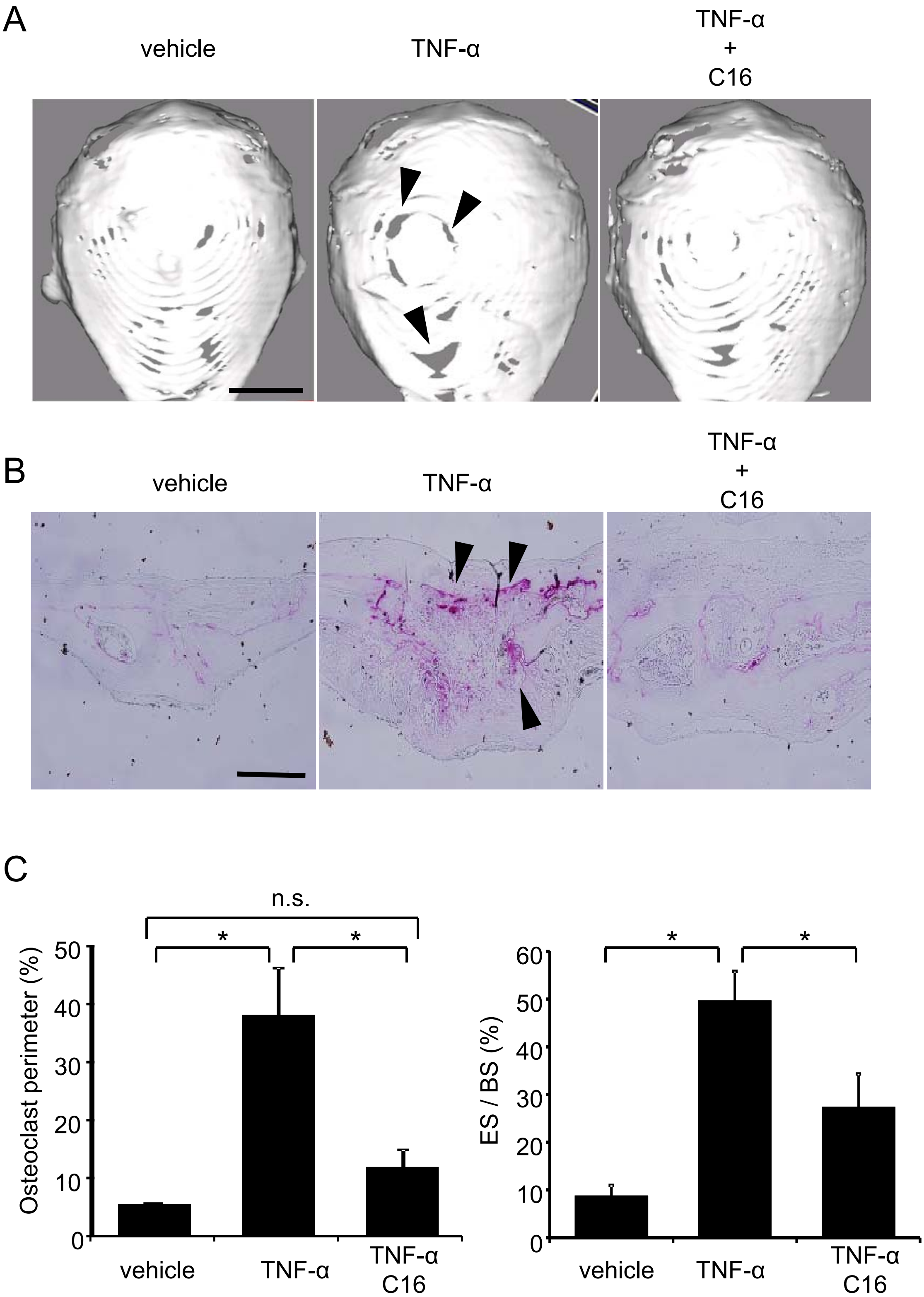
A
vehicle
TNF-α
TNF-α
+
C16
B
vehicle
TNF-α
TNF-α
+
C16
C
n.s.
*
*
Osteoclast perimeter (%)
0
10
20
30
40
50
vehicle
TNF-α
TNF-α
C16
*
*
ES / BS (%)
0
10
20
30
40
50
60
vehicle
TNF-α
TNF-α
C16